SLAC-PUB-3227
September 1983
(A)

HIGH PULSE POWER RF SOURCES FOR LINEAR COLLIDERS*

P. B. Wilson
Stanford Linear Accelerator Center
Stanford University, Stanford, California 94305

Introduction

RF sources with high peak power output and relatively short pulse lengths will be required for future high gradient e^+e^- linear colliders. The required peak power and pulse length depend on the operating frequency, energy gradient and geometry of the collider linac structure. The frequency and gradient are in turn constrained by various parameters which depend on the beam-beam collision dynamics, and on the total ac "wall-plug" power that has been committed to the linac rf system. Because the beam-beam, rf source and accelerating structure parameters are interwoven in a rather complex way, it will be useful to review first some of the basic expressions for linear collider design. These will lead in turn to specific rf source requirements. In particular, we will first want to see how the required rf source parameters (peak power, pulse length, repetition rate) scale as a function of frequency. In the sections that follow, various rf sources which might meet these requirements are reviewed. Existing source types (e.g. klystrons, gyrotrons) and sources which show future promise based on experimental prototypes are first considered. Finally, several proposals for high peak power rf sources based on unconventional concepts are discussed. These are an FEL source (two beam accelerator), rf energy storage cavities with switching, and a photocathode device which produces an rf current by direct emission modulation of the cathode.

Linear Colliders

The basic expressions giving the luminosity per collision $\mathcal{L}_1$, the disruption parameter D, the pinch enhancement factor $H(D)$ and the beamstrahlung parameter for a linear collider are well known. We take them in the form given by Wiedemann,[1] but with some modifications and restrictions proposed by Richter.[2] First, a round beam is assumed; second, the average energy loss per particle from beamstrahlung as given in Ref. 2 for Gaussian bunches is reduced by the factor $2\sqrt{2}$ to obtain an rms energy spread in the center-of-mass frame of the colliding beams; third, this beamstrahlung spread, σ_ϵ, is enhanced by the same factor, $H(D)$, by which the luminosity is increased. With these modifications, the expressions for $\mathcal{L}_1$, D and σ_ϵ can be manipulated to give the following useful secondary relations:

$$f_r(Hz) = 43\left[\frac{E_0(\mathrm{TeV})\cdot\mathcal{L}_1(10^{32})}{\sigma_z(mm)\cdot\sigma_\epsilon/E_0}\right] \qquad (1a)$$

$$N(10^{10}) = 41\left[\frac{\sigma_z^2(mm)\cdot\sigma_\epsilon/E_0}{E_0^2(\mathrm{TeV})\cdot D\cdot H(D)}\right] \qquad (1b)$$

$$\sigma^*(\mu m) = 0.76\left[\frac{\sigma_z^3(mm)\cdot\sigma_\epsilon/E_0}{E_0^3(\mathrm{TeV})\cdot D^2\cdot H(D)}\right]^{1/2} \qquad (1c)$$

$$P_b(MW) = 2.9\left[\frac{m\cdot\sigma_z(mm)\cdot\mathcal{L}_1(10^{32})}{D\cdot H(D)}\right] \quad . \qquad (1d)$$

Here f_r is the pulse repetition rate of the linac, N is the number of particles per bunch, σ^* is the rms transverse beam dimension, eE_0 is the energy per beam, σ_z is the bunch length, $P_b \approx eNE_0mf_r$ is the average power per beam (light beam loading), and m is the number of bunches accelerated during one linac pulse. Usually values for $\mathcal{L}_1$, E_0 and σ_ϵ/E_0 are specified a priori. Values for σ_z and D can then be chosen based on other considerations. In addition the operating frequency and accelerating gradient remain to be specified. Some factors which have a bearing on the choice of these parameters are briefly described in the following sections.

Beam Efficiency

The parameter k_1, which relates the stored energy per unit length, w, in an accelerating structure to the square of the accelerating gradient, E_a, can be written $k_1 = E_a^2/4w = C_s/\lambda^2$. The constant C_s depend on the geometry of the accelerating structure. It is a strong function of the ratio a/λ, where a is the radius of the beam hole opening. For a SLAC-type disk loaded structure with $v_g/c = .018$, $C_s = 2.0\times10^{11}$ V-m/C. The constant C_s varies approximately as $(a/\lambda)^{-1}$; the exact functional dependence for a disk loaded structure is given in Ref. 3. In the limit of light beam loading, the beam efficiency is given by $\eta_b \approx mqE_a/w = 4meNC_s/E_a\lambda^2$, where q is the charge per bunch. For the particular case of a disk loaded structure, this becomes in practical units,

$$\eta_b \approx 1.3\times10^{-3}\left[\frac{m\cdot N(10^{10})}{E_a(\mathrm{MV/m})\cdot\lambda^2(m)}\right] \quad . \qquad (2)$$

This expression assumes operation on the crest of the accelerating wave, ignores energy radiated by the bunches into higher-order modes (a good assumption for $m \gg 1$), and is valid only for η_b up to about 20%. See Ref. 4 for complete expressions without these restrictions.

Energy Sag Between Bunches

The long range, fundamental mode wake per bunch is $\Delta E_a(1) = 2k_1q$. Thus the total energy sag from the first to the last bunch is related to the efficiency by

$$\Delta E_a(\mathrm{tot})/E_a = m\Delta E_a(1)/E_a \approx \frac{1}{2}\eta_b \quad . \qquad (3)$$

For example, a train of 10 bunches with $\eta_b = 20\%$ gives $\Delta E_a(1) \approx 1\%$ and $\Delta E_a(\mathrm{tot}) \approx 10\%$.

Single Bunch Energy Spread

One of the most important considerations in the design of a linear collider is the energy spread within a single bunch. The final focus system must be able to focus this spread to the required submicron transverse beam dimensions. Also, if successive bunches are to be directed to different interaction regions, one would like the single bunch spread, $\Delta E(SB)$, to

* Work supported by the Department of Energy, contract DE-AC03-76SF00515.

Invited talk presented at the 12th International Conference on High Energy Accelerators,
Batavia, Illinois, August 11-16, 1983

ac power. The disruption parameter is adjusted so the energy sag between bunches is less than the total single bunch energy spread. Successive bunches in a given accelerator pulse can then be switched between different interaction regions using only a dc magnetic field. Then

$$\begin{aligned} \sigma_z &= .018 \quad (\sigma_z = 1.8 \text{ mm at } \lambda = 10 \text{ cm}) \\ E_a\lambda &= 2 \text{ MV} \quad (E_a = 20 \text{ MV/m at } \lambda = 10 \text{ cm}) \\ D &= 1.0 \\ H(D) &= 3.5 \end{aligned} \Big\} \text{ at } \lambda = 10 \text{ cm}$$

The above choices now lead to the following:

$$\begin{aligned} N/\lambda &= 38 \times 10^{10}\ m^{-1} \\ \Delta E(SB)/E_0 &= \text{const} = 1.2\% \ (\pm\ 0.6\%) \\ \eta_b &= \text{const} = 20\% \\ P_b &= \text{const} = 12 \text{ MV/beam} \\ P_{ac} &= \text{const} = 120 \text{ MW/beam} \\ E(m = 8) &= 0.90\, E_0 \ (1.3\% \text{ per bunch}) \end{aligned}$$

Efficiencies $\eta_s = \eta_{rf} = 0.7$ have been used, the latter assuming some improvement over present technology. The collider parameters at various wavelengths are summarized in Table I.

Table I

λ (cm)	10	5	2	1	Scaling
L/beam (km)	50	25	10	5	λ
E_a (MV/m)	20	40	100	200	λ^{-1}
σ_z (mm)	1.8	0.9	0.4	0.2	λ
N (10^{10})	3.8	1.9	0.8	0.4	λ
f_r (H_z)	240	480	1200	2400	λ^{-1}
D	1	0.75	0.5	0.3	$D \cdot H(D) \sim \lambda$
$H(D)$	3.5	2.4	1.4	1.2	
σ^* (μm)	0.31	0.18	0.09	0.06	$[\lambda \cdot H(D)]^{1/2}$

These results can now be applied to compute the required peak source power and pulse length as a function of wavelength. Again assume a copper disk loaded structure with $v_g/c = .018$ and an attenuation parameter $\tau = 0.4$. Such a structure has an efficiency $\eta_s = 0.7$ and a length $L_s = 3.0$ m at $\lambda = 10$ cm. Table II below shows rf parameters at various wavelengths for the case in which both τ and v_g/c are held constant. The Q and shunt impedance are 13,000 and 55 MΩ/m at $\lambda = 10$ cm, and scale as $\lambda^{1/2}$ and $\lambda^{-1/2}$ respectively.

Table II

λ (cm)	10	5	2	1	Scaling
E_a (MV/m)	20	40	100	200	λ^{-1}
L_s (m)	3.0	1.06	0.27	0.10	$\lambda^{3/2}$
$2a$ (mm)	24	12	4.8	2.4	λ
T_f (ns)	550	220	50	18	$\lambda^{3/2}$
No. Feeds (10^3)	17	24	37	53	$\lambda^{-1/2}$
$\hat{P}_{tot}$ (GW)	670	950	1500	2100	$\lambda^{-1/2}$
$\hat{P}$/feed (MW)	40	40	40	40	const.
$\hat{P}/m$ (MW/m)	13	38	150	420	$\lambda^{-3/2}$
W_{tot} (kJ/pulse)	370	190	75	37	λ
W/m (J/m/pulse)	7.5	7.5	7.5	7.5	const.

Suppose that one rf source supplies 8 feeds. Then the required peak power is 320 MW, the energy per pulse varies from 180 J at $\lambda = 10$ cm to 6 J at $\lambda = 1$ cm, and the total number of sources varies from 2100 up to 6600 over the same wavelength range. Using the repetition rates from Table I, the average power per source varies from 42 kW at 10 cm down to 13 kW at 1 cm.

RF Sources and Limitations

In the following sections we consider some high peak power rf sources which can meet the above requirements for driving a linear collider. The requirements on peak power, pulse length and repetition rate have already been discussed. Other factor to be considered are: frequency and amplitude stability, bandwidth, and the choice between oscillators and amplifiers. Narrow bandwidth amplifiers, usually klystrons, are used to drive the present generation of multisection linacs. However, other types of microwave sources which are normally operated as oscillators cannot be ruled out as drivers for high gradient colliders. First of all, oscillators can often be converted to amplifiers by some change in the configuration of the device, e.g. magnetrons to crossed field amplifiers, gyrotrons to gyroklystrons, etc. Secondly, oscillators can be operated as amplifiers by injection locking. Assuming that the frequency of the oscillator is determined by a resonance with central frequency ω_0 and bandwidth $BW = \omega_0/2Q_L$, the locking power P_i required at frequency $\omega_i = \omega_0 + \Delta\omega$ is[7] $P_i/P_0 = (\Delta\omega/BW)^2$, where P_0 is the output power. Practical experience with injection locking of magnetrons indicates that a minimum locking power on the order of -15 db with respect to the output power is required.[8] Even though this locking power is large compared to the drive power for a high gain klystron, the system efficiency including the drive power is reduced by only a few percent below the conversion efficiency of the oscillator itself.

Space Charge Limitations on Peak Power

A thorough investigation of the physical limitations on peak power, pulse length and repetition rate for each class of high power source will not be possible here. One important limitation on peak power, however, is worth noting. If an electron beam from a cathode is injected into a round metallic pipe, the current is limited by space charge depression at the center of the beam. The maximum current for a beam with voltage V_0 and radius r_b injected into a tube with radius r_w is[6,9]

$$\frac{I_{\max}}{17\ kA} \approx g(\gamma_0^{2/3} - 1)^{3/2} \quad , \tag{10}$$

where $\gamma_0 = 1 + (V_0/511\ kV)$, $g = [1 + 2\,\ell n(r_w/r_b)]^{-1}$ for a solid beam and $g = [2\,\ell n(r_w/r_b)]^{-1}$ for a hollow beam. The corresponding beam power is

$$\frac{P_{\max}}{8.7\ GW} \approx g(\gamma_0^{2/3} - 1)^{3/2}\,(\gamma_0^{1/3} - 1) \quad . \tag{11}$$

This is a fairly generous limit on power. For a solid beam with $r_b/r_w = 0.75$, $P_{\max} \approx 600$ MW and 2.6 GW at $V_0 = 500$ kV and 2 MV respectively.

be smaller than $\Delta E_a(1)$ above. For a Gaussian bunch in a SLAC-type disk loaded structure operating at 100 MV/m, the relative energy spread which contains 90% of the particles is given as a function of the number of particles per bunch in Fig. 1. In these plots the energy spread has been minimized by adjusting the phase of the bunch with respect to the crest of the accelerating wave. It is seen that below a certain critical value $N = N_c$ the energy spread is roughly equal to the zero current spread, which is due simply to the $\cos\theta$ variation in the accelerating wave over the length of the bunch. In this region

$$\Delta E(SB)/E_0 \approx 50\,(\sigma_z/\lambda)^2 \quad . \quad N < N_c \qquad (4)$$

The constant in the above expression does not depend strongly on the form of the bunch current distribution. It is nearly the same for a Gaussian, truncated Gaussian and rectangular distribution as long as the actual σ_z of the distribution is used (e.g. $\sigma_z = \ell_b/\sqrt{12}$ for a rectangular distribution of length ℓ_b). Above N_c the curves in Fig. 1 can be used to scale to other values of gradient and wavelength according to

$$\Delta E(SB)/E_0 = F[N/(E_a\lambda^2), \sigma_z/\lambda] \quad . \qquad (5)$$

These results are conservative, since by tailoring the shape of the current distribution it is in principle possible to reduce the energy spread below that for Gaussian bunches.

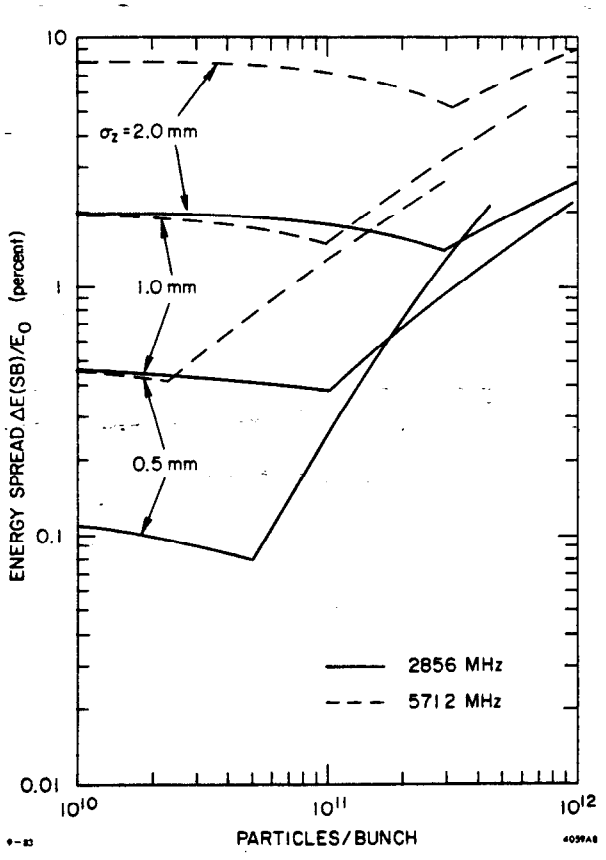

Fig. 1. Minimum single bunch energy spread (90% of particles) for a Gaussian bunch in the SLAC accelerating structure.

Transverse Emittance Growth

The transverse emittance growth in a collider due to the interaction of an off-axis beam of width σ_x with dipole modes will scale approximately as

$$\Delta\epsilon/\epsilon = (NW_\perp x_0 \bar{\beta}/\sigma_x E_a)^2 \qquad (6)$$

where x_0 is the off-axis distance, $W_\perp$ is the dipole wake function at the tail of the bunch and $\bar{\beta}$ is the average beta function for the focusing lattice. The wake function will depend on the bunch length, and will typically scale with the operating wavelength as $W_\perp(\sigma_z/\lambda) \sim \lambda^{-(3\pm(1/2))}$. Thus emittance growth is constant under the following scaling

$$\sigma_z \sim \lambda, \quad N \sim \lambda, \quad E_a \sim \lambda^{-1}, \quad \bar{\beta} \sim \lambda, \quad x_0 \sim \sigma_x \quad . \qquad (7)$$

Breakdown Limitation on Gradient

The breakdown limitation on the gradient in an accelerating structure will depend on the wavelength, the pulse length T_p, the ratio of the peak field on the surface to the average gradient, E_p/E_a, and perhaps on other details of the structure geometry and on the physical properties of the surface itself. From experience at SLAC, indications are that the breakdown gradient will lie in the range 50-100 MV/m for $\lambda =$ 10 cm, $E_p/E_a \approx 2$ and $T_p \approx 1$ μs. For shorter pulse lengths and higher frequencies the breakdown gradient should increase. Suppose E_b varies as $E_b \sim \omega^\alpha/T_p^\beta$. Experimental evidence concerning the value of α is sparse, but probably $0 < \alpha < 1$. Measurements[5] at SLAC on breakdown in klystron windows give $\beta \approx 1/3$. This is also in line with the variation in breakdown with pulse length for dc pulses applied to dielectrics.[6]

Wall Plug Power

The total ac power required per beam is $P_{ac} = P_b/(\eta_{rf}\eta_s\eta_b)$. Here η_{rf} is the efficiency for conversion of power from the ac lines to rf input at the structure, η_s is the efficiency for conversion of the rf input energy per pulse to useful stored energy in the structure [see for example, Ref. 3, Eq. (10.4)], and η_b is the beam efficiency given in Eq. (2). Combining Eqs. (1b), (1d) and (2),

$$P_{ac}(\mathrm{MW}) = \frac{54}{\eta_{rf}\,\eta_s}\left[\frac{\mathcal{L}_1(10^{32})\cdot E_0^2(\mathrm{TeV})\cdot E_a(\mathrm{MV/m})\cdot\lambda^2(m)}{\sigma_z(mm)\cdot\sigma_\epsilon/E_0}\right]. \qquad (8)$$

Note that $P_{ac} \sim E_a\lambda/(\sigma_z/\lambda)$. Thus both the total ac power and the single bunch energy spread, Eq. (5), are independent of wavelength if the following scaling is used:

$$\sigma_z \sim \lambda \quad , \quad E_a \sim \lambda^{-1} \quad , \quad N \sim \lambda \quad . \qquad (9)$$

This scaling also agrees with Eq. (7) for transverse emittance growth. Note that the disruption parameter is a free parameter that can be used to adjust σ^*, P_b and N. It has no effect on P_{ac}.

Scaling with Frequency

The expressions in the previous sections can now be applied to show how typical collider and rf source parameters scale with frequency. As an example, take the following basic parameters: $E_0 = 1$ TeV, $\sigma_\epsilon/E_0 = 0.1$, $m = 8$, $\mathcal{L}_1 = 1.0 \times 10^{32}\ cm^{-2}s^{-1}$, $\mathcal{L}_{tot} = 8 \times 10^{32}\ cm^{-2}s^{-1}$. The bunch length is now chosen to give a reasonable single bunch energy spread. The gradient is set consistent with reasonable total

Survey of Conventional Sources

Klystrons

There are no fundamental limitations which prevent klystrons from being scaled to produce peak powers of at least several hundred megawatts. Some years ago, in fact, a klystron with a very short pulse length ($\approx$ 15 ns) operating at 3.35 GHz was built[10] with a design peak power of 1 GW (at $V_0 = 1$ MV, $I_0 = 2$ kA and $\eta = 50\%$). However, the tube failed before it could be tested at full output power and the development was not persued further. At SLAC there is a program to developed a klystron with a peak power of 150 MW at a pulse length of 1 μs and a repetition rate of 180 pps. The design beam voltage, beam current and efficiency are 450 kV, 600 A and 55% respectively. Recently, an experimental tube in this program has produced a peak power exceeding 100 MW at the design pulse length, although at reduced repetition rate and with an efficiency of about 45%. It is expected that improvements in focusing will increase the peak power and efficiency toward the design goals.

Gyrotrons and Gyroklystrons

In the gyrotron, electrons rotating in orbits at the cyclotron frequency do work against the transverse rf electric field of a TE mode in a smooth cylindrical waveguide. Because a slow-wave structure is not required, the gyrotron oscillator is normally considered to be a source for high CW power at millimeter wavelengths (see review by V. L. Granatstein *et al.*[12]). However, a pulsed gyrotron at the Tomsk Polytechnic Institute[13] has delivered 1.4-2 GW at 3 GHz with a beam voltage of 900 kV, a beam current of 8 kA, a pulse length of 60 ns and a maximum efficiency of 30%. See also the review in Ref. 14.

The amplifier version of the gyrotron, the gyroklystron, has received less attention. Operation of a gyroklystron as a high peak power source in the 1-10 cm wavelength range would have certain advantages. The solenoid providing the longitudinal magnetic field could be normal conducting at longer wavelengths. The dimensions of the high power output cavity for a gyroklystron are large compared to a klystron at the same wavelength, minimizing breakdown and beam interception problems. However, there are several problems: a mode converter, which could be subject to breakdown problems, is needed in the output guide; it may be difficult to attain an efficiency equal to that of a well-designed klystrons; and finally, space charge limitations on estimate peak power are more severe because a substantial fraction of the beam energy is in the transverse orbital motion.

Backward Wave Oscillators

A high current, high energy beam injected into an appropriate slow wave structure can produce a high peak rf output power, usually through the mechanism of backward wave amplification along the structure. Output powers in the range 100-1000 MW at frequencies in the range 3-10 GHz have been reported,[14,15] with efficiencies up to $\approx$30% and pulse lengths of 20-40 ns.

Crossed Field Devices

Very high peak powers (e.g. 1.7 GW at 3 GHz with $T_p = 30$ ns and $\eta = 35\%$[16]) have been reported for relativisitic magnetrons. However, these devices are basically oscillators (although in principle they can be phase locked), and in addition pulse lengths tend to be short ($<$ 50 ns) because of cathode back bombardment and anode plasma sheath formation.

Several variations of the magnetron, which might overcome some of these limitations, are of interest. In the gyromagnetron[17] a hollow beam is injected parallel to the axis of a coaxial structure with slotted inner and outer walls. The rippled-field magnetron[18] replaces the slotted metallic anode structure of the magnetron with an azimuthally periodic magnetic field. The crossed field amplifier is of obvious interest as a source for accelerators, although the development of this device so far has not been pursued in the direction of high peak power.

Unconventional Sources

Virtual Cathode Oscillator

In the simplest of these devices, a hollow beam having a current which is above the space charge limit given in Eq. (10) is injected into a cylindrical waveguide. An oscillating virtual cathode forms at the mouth of the waveguide, the frequency of the oscillation being given approximately by the relativistic plasma frequency. In a recent review, Sullivan[19] lists virtual cathode oscillators (vircators) which have produced peak powers up to 3 GW. However, these devices tend to have rather low efficiencies and produce a broad bandwidth output. The highest efficiency (12%) is reported for a reflex triode, which produced 1.4 GW at a frequency 3.3 GHz.

A variation of the virtual cathode oscillator is the relativistic electron beam device of Friedman *et al.*[20] In this device a high current beam is injected into a cylindrical beam pipe with two or more gaps. Virtual cathodes form at the gaps, and electrons circulating back and forth between the gaps produce a deep modulation in the dc beam at a frequency determined by the gap spacing. A current modulation of 100% has been attained[20] for a 7 kA, 700 kV (5 GW) beam with a pulse width of 120 ns at frequencies of 280 and 750 MHz. This modulated beam could be put through an rf output circuit to extract rf power at high efficiency.

Two Beam Accelerator

In the two beam accelerator,[21,22] a high current low voltage electron beam runs parallel to the low current, high voltage beam to be accelerated. RF energy is alternately removed from the high current beam by FEL sections and restored by induction linac modules. An FEL operating at a wavelength of 1 cm could provide a power of 500 MW/m at a pulse width of 50 ns and an efficiency of 71%.[22] From Table II, this could power a collider operating at this wavelength to a gradient exceeding 200 MV/m.

Pulse Compression

Several schemes have been devised to convert the energy in an rf pulse with long pulse length and relatively low peak power to a shorter pulse length with a higher effective peak power. One such technique, SLED[23] (SLAC Energy Development), is now operational at SLAC. In SLED, high-Q resonant cavities store energy during a large fraction of each klystron pulse, then discharge this energy into the accelerator in a much shorter time (equal to the accelerator filling time) during the final part of the pulse. During this discharge period, which is triggered by a 180° phase reversal in the wave coming from the klystron,

power flowing from the storage cavities adds coherently to the direct power from the klystron. The principle advantage of SLED is that it is achieved entirely by passive components: two high-Q resonators, a 3 db hybrid and a low power phase shifter in the input drive to the klystron.

An over coupled resonant cavity is already a simple pulse compressor. At the instant the generator driving such a cavity is switched off, the wave emitted from the cavity has a field strength which is up to twice that in the incident wave from the generator. If the phase of the generator wave is now reversed instead of being switched off, the additional field adds to the wave from the resonator to give a field strength which is up to three times that of the incident wave, equivalent to nine times the incident power. Two cavities together with a 3 db coupler allow the power reflected from the storage cavities to be directed toward an accelerator rather than flowing back toward the klystron. The effective power gain in a practical situation is always considerably less than nine because of losses in the storage cavities and limitations on the available klystron pulse length. At SLAC in the SLED mode, an energy enhancement ratio of 1.40 is reached for a klystron pulse length of 2.5 μs and an accelerator filling time of 0.83 μs. The compression efficiency is then $(1.40)^2(0.83/2.5) = 0.65$. If the pulse length is increased to 5.0 μs, the enhancement ratio increases to 1.78, but the compression efficiency falls to 52%. The energy enhancement as a function of klystron pulse length is shown in Fig. 2 for the SLAC accelerating structure, where Q_0 is the unloaded Q of the storage cavities. Expressions for the energy enhancement factor for constant gradient and constant impedance structures are given in Refs. 23 and 24 respectively.

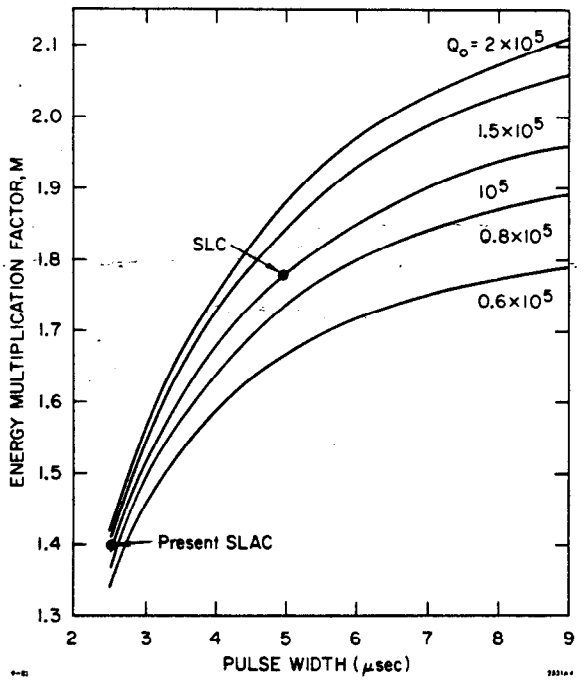

Fig. 2. SLED energy enhancement ratio as a function of pulse length for the SLAC constant gradient structure.

In another form of pulse compression, illustrate schematically in Fig. 3, an active switch in the high power output waveguide from an energy storage cavity is used to trigger the discharge of energy from the cavity into an accelerator section. The enhancement ratio in the accelerating gradient is given by $M = [(T_p/T_s)\eta_c\eta_s]^{1/2}$, where T_p is the klystron pulse length, T_s is the structure filling time, and η_c and η_s are the efficiencies for transfer of energy from the klystron pulse to the storage cavity and from the cavity to the accelerating structure. For typical parameters the net pulse compression efficiency $\eta_c\eta_s$ is on the order of 40%. Detailed expressions for η_c and η_s are given in Ref. 25.

The critical component in this pulse compression method is the high power switch. In the system shown in Fig. 3, an electron density on the order of $10^{14}/\text{cm}^3$ must be achieved in a column across the waveguide with an area on the order of 0.1 cm^2 for good switching efficiency. By triggering a discharge in a high pressure gas, Alvarez *et al.*[26] have switched a peak power of 160 MW with a gain in peak power of 23 and a compression efficiency of about 10%. They have also proposed an improved switching mechanism based on a low pressure plasma discharge.

An alternative form for a high power switch could be based on producing a phase shift, rather than a reflection, in the high power waveguide. Initial calculations indicate that a broad area electron beam (perhaps from a photocathode) over an area on the order of $\lambda^2/4$ could give an adequate phase shift at moderate current densities (< 50 A/cm^2) with good switching efficiency ($> 95\%$). The beam would need to be directed normal to the rf electric field, and would probably need to be guided by a magnetic field of a few kilogauss.

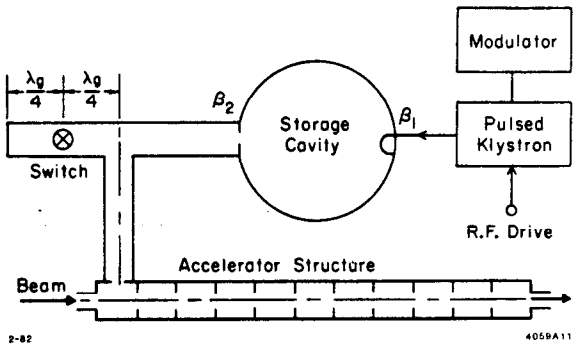

Fig. 3. RF pulse compression using an energy storage cavity with switching.

Photocathode Microwave Source

An rf source based on illuminating a photocathode with an intensity modulated laser beam has been described previously.[25] The chief advantage of this device is that electron bunches which are short compared to the rf wavelength are formed directly at the cathode. After acceleration to a high potential and compression in lateral dimesions, the bunches are put through an output circuit (similar to the output cavity of a klystron) to extract rf power. If the phase and energy spread within the bunch have not been substantially increased by space charge forces, all the electrons in each bunch can be brought nearly to rest if the amplitude of the rf field in the output circuit

is adjusted to be equal to the dc voltage. The efficiency can therefore approach 100% in principle. Another advantage of this device is that a simple dc supply may sufficient to drive the cathode; an expensive and often inefficient high voltage, high current pulser is not needed. The photocathode acts as a gate to convert dc energy directly into microwave pulses.

The chief limitation on the performance of the photocathode source is the increase in the energy spread in the bunch due to space charge. If we take a simple model in which the bunch is compressed uniformly in radius during acceleration, assuming also that the bunch length is small compared to the bunch radius, then the output power is calculated to be

$$P_0 \approx \pi \left(\frac{r_0}{\lambda}\right)\left(\frac{r_c}{L}\right)\left(\frac{\Delta V}{V_0}\right)\cdot\frac{V_0^2}{Z_0} \qquad (12)$$

where r_0 is the beam radius at the output cavity gap, r_c is the cathode radius, L is length of the accelerating region, ΔV is the allowable space charge spread and $Z_0 = 377\ \Omega$. Setting $r_c = L$, $r_0 = 0.2\ \lambda$ and $\Delta V/V_0 = 0.3$ (which still allows an efficiency greater than 95%), the output power is about 125 MW at $V_0 = 500$ kV and 500 MW at $V_0 = 1$ MV. In this example, the average current density at the cathode is 6 A/cm^2 (peak current density ≈ 60 A/cm^2) for $L = 5$ cm and $V_0 = 1$ MV.

The wall-plug power for the laser is given by $P_\ell/P_0 \approx \phi_w/(V_0\eta_q\eta_\ell)$, where ϕ_w is the work function, η_q is the quantum efficiency and η_ℓ is the laser efficiency. For typical parameters ($\phi_w = 5$ eV, $\eta_q = 0.1$, $\eta_\ell = 0.01$, $V_0 = 1$ MV), the required laser wall-plug power is less than 1% of the rf output power. Eventually it may be possible to dispense with the laser entirely. Rapid advances are being made toward solid state cathodes which can emit electrons directly under the action of a small control voltage.

Acknowledgements

The author regrets that it was not possible to give more complete references and background for the calculations, devices and concepts presented in this brief review. Discussions on linear colliders with many colleagues have been helpful. In addition the author would like to thank: A. Drobot (high power sources); G. Farney (crossed field amplifiers); M. Chodorow and Z. D. Farkas (injection locking); C. K. Sinclair, W. Herrmannsfeldt and F. S. Felber (photocathode rf source); D. L. Birx and R. O. Hunter (switches for high power rf).

References

1. H. Wiedemann in *Proc. of the Summer Institute on Particle Physics*, Stanford Linear Accelerator Center, Stanford, California, July 1981, p. 313 (also SLAC Report 245, January 1982).
2. B. Richter, "SLC and Future Linear Colliders," this conference.
3. P. B. Wilson in *Physics of High Energy Particle Accelerators*, R. A. Carrigan, F. R. Huson and M. Month ed. (AIP Conference Proceedings No. 87, American Institute Physics, New York, 1982), p. 527.
4. *Ibid.* pp. 531, 544.
5. G. Konrad, private communication.
6. J. A. Nation, Part. Accel. 10, 1 (1979).
7. R. Adler, Proc. IEEE 61, 1380 (1973).
8. M. Chodorow, private communication.
9. R. B. Miller, *Intense Charged Particle Beams* (Plenum Press, New York, 1982), Sec. 3.3.
10. Rome Air Development Center, Report No. RADC-TR-70-101 (July 1970).
11. G. Konrad, private communication.
12. V. L. Granatstein, M. E. Read and L. R. Barnett, IEEE Trans. Nucl. Sci. NS – 28, No. 3, 2733 (1981).
13. A. N. Didenko *et al.*, Sov. J. Plasma Phys. 2, 283 (1976).
14. L. S. Bogdankevich, M. V. Kuzelev and A. A. Rukhadze, Sov. Phys. Usp. 24, 1 (1981).
15. A. S. El'chaninov *et al.*, Sov. Tech. Phys. Lett. 6, 191 (1980).
16. G. Bekefi and T. J. Orzechowski, Phys. Rev. Lett. 37, 379 (1976).
17. C. D. Striffler *et al.*, IEEE Trans. Nucl. Sci. NS – 30, No. 4, 3429 (1983).
18. G. Bekefi, Appl. Phys. Lett. 40, 578 (1982).
19. Donald J. Sullivan, IEEE Trans. Nuc. Sci. NS – 30, No. 4, 3426 (1983).
20. M. Friedman, V. Serline, A. Drobot and L. Seftor, Phys. Rev. Lett. 50, 1922 (1983).
21. A. M. Sessler in *Laser Accelerator of Particle*, P. J. Channell ed. (AIP Conference Proceedings No. 91, American Institute Physics, New York, 1982), pp. 183-189.
22. D. Prosnitz, IEEE Trans. Nucl. Sci. NS – 30, No. 4, 2754 (1983).
23. Z. D. Farkas, H. A. Hogg, G. A. Loew and P. B. Wilson, Proceedings of the 9th International Conference on High Energy Accelerator, Stanford Linear Accelerator Center, Stanford, California, May 1974, p. 576.
24. Ref. 3, p. 550
25. P. B. Wilson, IEEE Trans. Nucl. Sci. NS – 28, No. 3, 2742 (1981). Also Ref. 3, p. 551.
26. R. A. Alvarez, D. L. Birx, D. P. Byrne and E. J. Lauer, Part. Accel. 11, 125 (1981).